

# Chapter 2

## Model Development for Air Conditioning System in Heavy Duty Trucks

J.T.B.A. Kessels and P.P.J. van den Bosch

**Abstract** This chapter presents a modelling approach for the air conditioning (AC) system in heavy duty trucks. The presented model entails two major elements: a mechanical compressor model and a thermal AC model. The compressor model describes the massflow of the refrigerant as well as the mechanical power requested from the combustion engine. The thermal AC model predicts how ambient air flow cools down when it passes the AC system. This model also includes the latent heat emerging from water condensation. Both elements of the model have been validated with experimental data. The compressor parameters follow from hardware-in-the-loop experiments where the AC compressor is measured under various load profiles. Validation of the thermal AC model is done by climate chamber testing with a DAF XF heavy duty truck on a roller dynamometer.

**Keywords** Lumped-parameter modeling • Air conditioning system • Automotive

### 2.1 Introduction

Heavy duty long haul trucks are typically equipped with an air conditioning (airco) system to offer a comfortable cabin climate to the driver. The airco system fulfills two elementary functions: cooling down the cabin temperature (when the ambient temperature is too high) and dehumidifying the air (in rainy conditions or winter weather). Both functions request mechanical power which is ultimately delivered by the internal combustion engine (ICE). This chapter presents a modeling approach for the mechanical power consumption of the airco compressor. Furthermore, it also presents a model for the thermal behavior of the airflow when it is cooled down by the airco system. These models can be used to develop advanced control strategies for improving the energy efficiency of the airco system, see, for example, [4, 5].

---

J.T.B.A. Kessels (✉)

DAF Trucks N.V., Vehicle Control Department, Eindhoven, The Netherlands

e-mail: [John.Kessels@daftrucks.com](mailto:John.Kessels@daftrucks.com)

P.P.J. van den Bosch

Eindhoven University of Technology, Control Systems - Department of Electrical Engineering

e-mail: [P.P.J.v.d.Bosch@tue.nl](mailto:P.P.J.v.d.Bosch@tue.nl)



**Fig. 2.1** DAF XF prototype truck developed in CONVENIENT project

More specifically, an energy management strategy can incorporate these models to optimize the power demand of the airco system such that:

- the airflow towards the cabin receives exactly enough cooling power to establish the desired temperature and humidity for the driver;
- regenerative braking energy is stored in the thermal buffer capacity of the airco system.

This research is carried out within the EU collaborative project CONVENIENT<sup>1</sup> (Complete Vehicle Energy-saving Technologies for Heavy-Trucks, [2]). In this project a suite of technologies is developed to maximize the fuel economy of long haul trucks. In total three prototype trucks are developed to demonstrate these technologies. DAF Trucks N.V. is responsible for the development of the DAF XF tractor with semi-trailer, suitable for long haul applications, see Fig. 2.1. For this prototype truck with hybrid electric powertrain, smart auxiliaries are developed by means of a Smart Vehicle Powernet control concept [7]. The airco system of the truck is one of the auxiliaries considered in the Smart Vehicle Powernet. This chapter describes the underlying airco model for developing the Smart Vehicle Powernet [7].

<sup>1</sup>This work has received funding from the European Union's Seventh Framework Programme for research, technological development, and demonstration under grant agreement no [312314].

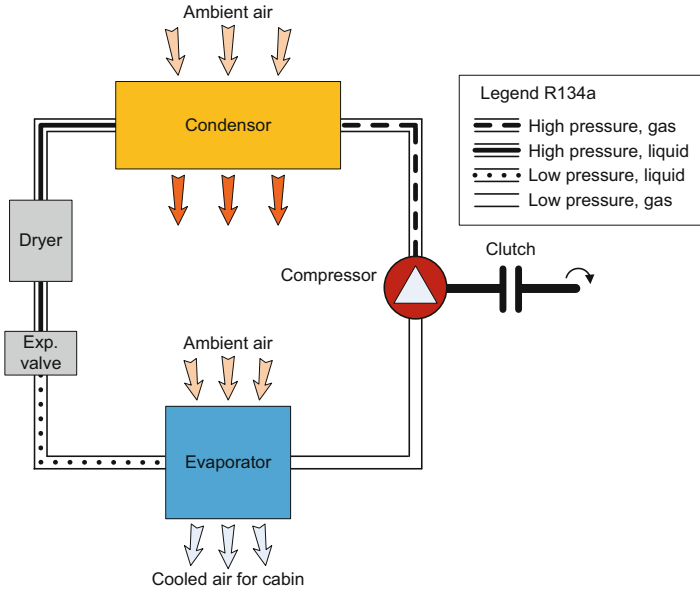


**Fig. 2.2** Overview of air conditioning system in heavy duty truck

## 2.2 System Overview

The basic principles of an air conditioning system are explained by thermodynamics, see, for example, [1]. A schematic overview of the air conditioning system in the truck is depicted in Fig. 2.2. This system circulates refrigerant R134a using the following hardware:

- **Compressor:** The compressor increases the pressure of the refrigerant. The compressor is belt driven and receives power from the ICE. A mechanical clutch is installed to (dis-)connect the compressor (from)/to the belt.
- **Condensor:** The condensor operates as a heat exchanger. It cools down the high pressure refrigerant and releases its heat to the airflow through the condensor. Cooling down the refrigerant leads to condensation of the refrigerant. The condensor is placed in the engine bay directly behind the grill to receive sufficient airflow.
- **Expansion valve:** The expansion valve releases the refrigerant towards the evaporator. This is a sensitive task because the influx should be balanced with the heat exchanged in the evaporator. Only gaseous refrigerant is allowed to leave the evaporator. Therefore the expansion valve monitors the refrigerant output from the evaporator to decide if more/less refrigerant has to flow into the evaporator.
- **Evaporator:** The evaporator is mounted in the Heating Ventilation and Air Conditioning (HVAC) system. The evaporator exchanges heat between the refrigerant

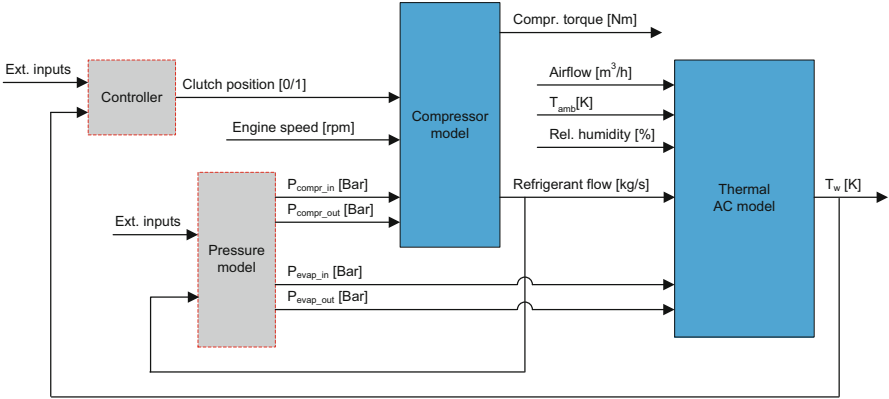


**Fig. 2.3** Cascade model structure for AC system

and the airflow which is used for cabin heating and ventilation. Refrigerant that flows through the evaporator absorbs heat from the airflow. The airflow cools down (and possibly also dehumidifies) and the refrigerant expands from liquid to gaseous phase. The airflow is directed further to the cabin for climate control.

The model developed in this work for the air conditioning system consists of two parts:

- **Compressor model:** A mechanical model for the compressor is constructed. This model translates mechanical power (delivered by the ICE) into cooling power (delivered to the refrigerant).
- **Thermal AC model:** This model describes the thermodynamic behavior of the air conditioning (AC) system. The main focus of this model is to describe the heat transfer in the evaporator. The evaporator is located in the HVAC system. The refrigerant in the evaporator will absorb heat from the air that flows through the HVAC. The main output from this model is an estimate of the temperature of the airflow downstream the evaporator.

Both models can be connected in a cascade structure, as visualized in Fig. 2.3. The underlying idea is to construct a simulation environment which is suitable for developing advanced HVAC controls. The output from the thermal AC model is used to evaluate driver comfort, whereas the compressor torque yields insight in the power demand of the airco system. A missing element in the model is the pressure model. This is planned for future research, but the interested reader could examine [10] for an example in passenger car application.

## 2.3 Compressor Model

The compressor model is based on two key parameters: volumetric efficiency and isentropic efficiency. The volumetric efficiency will be used to estimate the flow of the refrigerant through the compressor. The isentropic efficiency is used to estimate the mechanical power demand of the compressor. Both parameters have been measured by the supplier of the compressor on a hardware-in-the-loop (HIL) test bench for various pressure levels.

### 2.3.1 Calculation of Refrigerant Flow

The volumetric efficiency  $\eta_{\text{vol}}$  [-] is defined as the ratio of the actual measured flow  $\phi_a$  [m<sup>3</sup>/s] (measured at the suction side of the compressor at a certain pressure) and the theoretical flow  $\phi_t$  [m<sup>3</sup>/s]

$$\eta_{\text{vol}} = \frac{\phi_a}{\phi_t} \quad (2.1)$$

The theoretical flow  $\phi_t$  [m<sup>3</sup>/s] of a compressor can be calculated by multiplying its displacement volume  $V_p$  [m<sup>3</sup>] with its rotational velocity  $N$  [rpm]

$$\phi_t = \frac{N}{60} V_p \quad (2.2)$$

Given the density  $\rho$  [kg/m<sup>3</sup>] of the refrigerant at the suction side of the compressor, the actual refrigerant massflow  $\dot{m}_R$  [kg/s] is calculated as

$$\dot{m}_R = \rho \phi_a = \rho \eta_{\text{vol}} \frac{N}{60} V_p \quad (2.3)$$

### 2.3.2 Calculation of Compressor Power

The enthalpy of the refrigerant changes when it passes the compressor. This enthalpy change is used to define the isentropic efficiency. Considering an isentropic compressor, the theoretical work  $W_{\text{isen}}$  [J] done by the compressor is defined as

$$W_{\text{isen}} = - \int_{p_s}^{p_d} V dp \quad (2.4)$$

where refrigerant is compressed from pressure  $p_s$  [Pa] to  $p_d$  [Pa] (i.e., from the compressor suction side to the discharge side). The analytical solution for this integral is well known from literature, see, e.g., [9]

$$W_{\text{isen}} = \frac{\gamma}{\gamma - 1} m_R R_R T_s \left[ \left( \frac{p_d}{p_s} \right)^{\frac{\gamma-1}{\gamma}} - 1 \right] \quad (2.5)$$

with  $T_s$  [K] the temperature of the refrigerant at the suction side of the compressor.  $\gamma = 1.2$  [-] is the heat capacity ratio;  $R_R$  [J kg<sup>-1</sup> K<sup>-1</sup>] is the specific gas constant of the refrigerant and  $m_R$  [kg/mol] is the molecular weight of the refrigerant.

The isentropic efficiency  $\eta_{\text{isen}}$  [-] is defined as the ratio between the isentropic compressor work and the actual compressor work

$$\eta_{\text{isen}} = \frac{W_{\text{isen}}}{W_{\text{actual}}} \quad (2.6)$$

Given the isentropic efficiency, the actual mechanical energy demand from the compressor is calculated

$$W_{\text{actual}} = \frac{1}{\eta_{\text{isen}}} \frac{\gamma}{\gamma - 1} m_R R_R T_s \left[ \left( \frac{p_d}{p_s} \right)^{\frac{\gamma-1}{\gamma}} - 1 \right] \quad (2.7)$$

The mechanical compressor power  $P_{\text{AC}}$  [W] follows by replacing the refrigerant weight with the massflow from (2.3). This substitution holds for steady state conditions and results in

$$P_{\text{AC}} = \frac{1}{\eta_{\text{isen}}} \frac{\gamma}{\gamma - 1} \dot{m}_R R_R T_s \left[ \left( \frac{p_d}{p_s} \right)^{\frac{\gamma-1}{\gamma}} - 1 \right] \quad (2.8)$$

Finally, the compressor torque  $\tau_{\text{AC}}$  [Nm] is calculated with help of the rotational speed  $N$  [rpm]

$$\tau_{\text{AC}} = P_{\text{AC}} \frac{60}{2\pi N} \quad (2.9)$$

## 2.4 Thermal AC Model

The thermal AC model describes the transfer from AC cooling power into cold air out of the HVAC. The evaporator in the HVAC takes a central role here. Based on first principles of conduction and convection, its thermal behavior will be derived. There should be noted, however, that the humidity of the ambient air also plays an

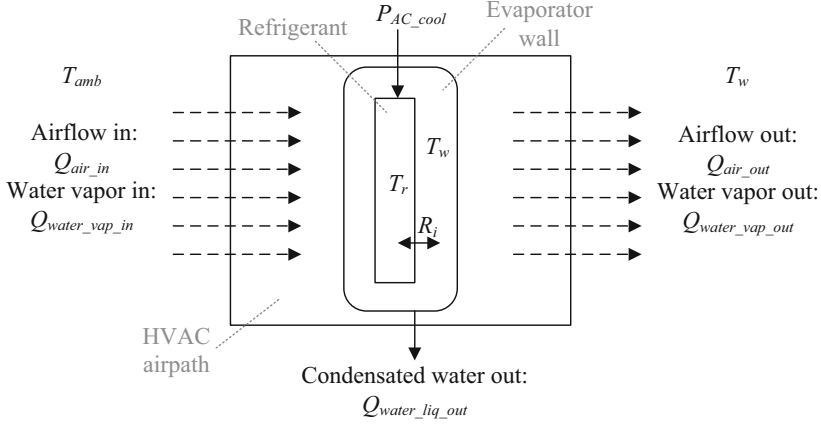


**Fig. 2.4** Thermal AC model

important role. After all, cold air can hold less water so cooling down ambient air in the HVAC easily results in condensation of water. This water drops out of the HVAC and incorporates the so-called latent heat which needs to be taken into account too.

### 2.4.1 Thermal Model Structure

The basic thermal model structure is depicted in Fig. 2.4. It is decided to model the heat exchanger of the evaporator as a lumped thermal mass with temperature  $T_w$  [K] (which refers to the wall temperature of the evaporator). Besides the temperature of the evaporator, the thermal model incorporates also the temperature of the refrigerant inside the evaporator:  $T_r$  [K]. The model injects cooling power  $P_{AC\_cool}$  [W] directly in the refrigerant. Furthermore, a thermal resistance  $R_i$  [K/W] is introduced to model the heat transfer  $Q_{w2r}$  [W] from evaporator to refrigerant

$$Q_{w2r} = \frac{T_w - T_r}{R_i} \quad (2.10)$$

Altogether, the thermal AC model resembles two thermal buffers

$$\begin{aligned} C_w \dot{T}_w = & Q_{air\_in} + Q_{water\_vap\_in} - Q_{air\_out} - Q_{water\_vap\_out} \\ & + Q_{latent} - Q_{w2r} \end{aligned} \quad (2.11)$$

$$C_r \dot{T}_r = Q_{w2r} - P_{AC\_cool} \quad (2.12)$$

with  $C_w$  [J/K] and  $C_r$  [J/K] the lumped heat capacity of the evaporator and refrigerant, respectively. The other terms will be described in the text below.

Ambient air with temperature  $T_{\text{amb}}$  [K] enters the HVAC with flow  $\phi_{\text{air}}$  [m<sup>3</sup>/s], specific heat  $c_{\text{air}} = 1005$  J/kg K, and density  $\rho_{\text{air}} = 1.25$  kg/m<sup>3</sup>. This leads to the heatflow  $Q_{\text{air\_in}}$  [W]

$$Q_{\text{air\_in}} = \rho_{\text{air}} c_{\text{air}} \phi_{\text{air}} T_{\text{amb}} \quad (2.13)$$

It is noted that the coefficients in (2.13) correspond to dry air. According to the relative humidity, however, the airflow will be a mixture of air and water vapor. This water vapor will result into an additional influx  $Q_{\text{water\_vap\_in}}$  [W] for the HVAC

$$Q_{\text{water\_vap\_in}} = c_{\text{water\_vap}} \phi_{\text{air}} X_{\text{air\_in}} T_{\text{amb}} \quad (2.14)$$

with  $c_{\text{water\_vap}}$  [J/kg K] the specific heat of water vapor and  $X_{\text{air\_in}}$  [kg/m<sup>3</sup>] the absolute humidity of ambient air. Further details on the calculation of  $X_{\text{air\_in}}$  will be provided in Sect. 2.4.2.

The airflow through the HVAC flows through the evaporator and cools down. It is assumed that the air temperature downstream the evaporator equals the wall temperature of the evaporator defined as  $T_w$  [K]. The corresponding heatflow  $Q_{\text{air\_out}}$  [W] of output air (dry) is equal to

$$Q_{\text{air\_out}} = \rho_{\text{air}} c_{\text{air}} \phi_{\text{air}} T_w \quad (2.15)$$

Similar as with the air–water mixture for the input flow, the heatflow corresponding to the water vapor leaving the HVAC is modeled as  $Q_{\text{water\_vap\_out}}$  [W]

$$Q_{\text{water\_vap\_out}} = c_{\text{water\_vap}} \phi_{\text{air}} X_{\text{air\_out}} T_w \quad (2.16)$$

with  $X_{\text{air\_out}}$  [kg/m<sup>3</sup>] the absolute humidity of the airflow leaving the HVAC. Note that this absolute humidity is equal or lower than the humidity of the input air. This is a side effect of cooling down the airflow. The underlying model equations for  $X_{\text{air\_in}}$  and  $X_{\text{air\_out}}$  will be provided in Sect. 2.4.2. A lower output humidity results in water condensation. Water droplets will flow out of the HVAC. The corresponding heatflow from liquid water leaving the HVAC is defined as  $Q_{\text{water\_liq\_out}}$  [W]

$$Q_{\text{water\_liq\_out}} = c_{\text{water\_liq}} \phi_{\text{air}} (X_{\text{air\_in}} - X_{\text{air\_out}}) T_w \quad (2.17)$$

with  $c_{\text{water\_liq}}$  [J/kg K] the specific heat of liquid water. Condensation of water vapor results in substantial heat. This so-called latent heat is also taken into account by means of  $Q_{\text{latent}}$  [W]

$$Q_{\text{latent}} = H_{\text{vap}} \phi_{\text{air}} (X_{\text{air\_in}} - X_{\text{air\_out}}) \quad (2.18)$$

with  $H_{\text{vap}} = 2257\text{e}3$  J/kg the specific heat of vaporization of water.



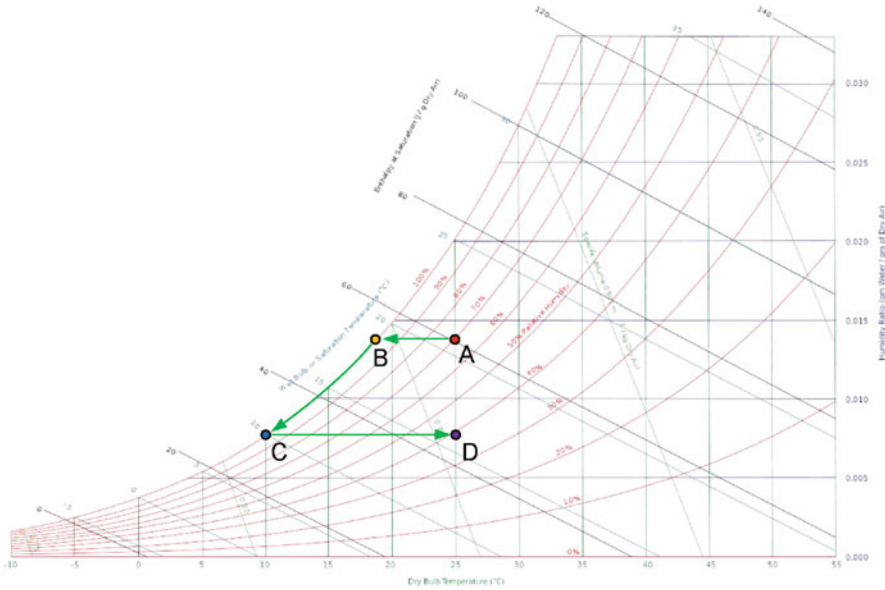


**Fig. 2.5** Psychrometric chart with visualization how air dehumidifies in HVAC

### 2.4.2 Air Humidity and Latent Heat

One aspect of an air conditioning system is that it cools down the air towards the cabin. A second aspect of the air conditioning system is that it also reduces the humidity of the air. This is because cold air cannot hold as much water vapor as warm air. How the model calculates the amount of water condensation in the HVAC, as well as the related heatflow  $Q_{\text{latent}}$ , is described in this section.

The psychrometric chart in Fig. 2.5 visualizes how the relative humidity changes under variation of temperature. As an illustrative example, consider a warm but rainy day with ambient temperature  $T_{\text{amb}} = 25^\circ\text{C}$  and relative humidity  $\text{RH} = 70\%$  (point A). By cooling down, the relative humidity increases up to  $\text{RH} = 100\%$  when reaching temperature  $T = 19^\circ\text{C}$  (point B). Remark: point B is called dewpoint because below this point, the air cannot contain more water vapor. Cooling down further will result in water condensation. Suppose that the air is further cooled down to  $T = 10^\circ\text{C}$  (point C). When this air is re-heated back to  $T = 25^\circ\text{C}$ , the relative humidity becomes approx.  $\text{RH} = 40\%$  (point D), which is substantially lower than the original humidity (point A) and helps preventing a foggy windscreen.

The report from Vaisala [6] is used as starting point for collecting the model equations for humidity conversion. The relative humidity  $\text{RH} [\%]$  of air is defined as the ratio of the water vapor pressure  $P_w [\text{Pa}]$  to the saturation water vapor pressure  $P_{ws} [\text{Pa}]$

$$\text{RH} = \frac{P_w}{P_{ws}} \times 100 \quad (2.19)$$

The saturation water vapor pressure  $P_{ws}$  typically relates to the situation where the air reaches  $RH = 100\%$ . The following approximation is proposed in [6]

$$P_{ws} = A \times 10^{\left(\frac{(T-273.15)m}{(T-273.15)+T_n}\right)} \quad (2.20)$$

with temperature  $T$  [K] and constants  $A = 611.6$ ,  $m = 7.591$ , and  $T_n = 240.7$  taken from [6]. The substitution of (2.20) in (2.19) allows to calculate  $P_w$  under the condition that  $RH$  is known.

From  $P_w$  the absolute humidity is calculated. The absolute humidity  $AH$  [g/m<sup>3</sup>] is defined as the mass of water vapor in a volume of 1 m<sup>3</sup> and calculated by [6]

$$AH = \frac{C \times P_w}{T} \quad (2.21)$$

with constant  $C = 2.167$  gK/J and  $T$  [K] the air temperature. Calculation of  $AH$  is done for point A and point C

$$AH_A = \frac{C \times P_w(T_A, RH_A)}{T_A} \quad (2.22)$$

$$AH_C = \frac{C \times P_w(T_C, RH_C)}{T_C} \quad (2.23)$$

with  $T_A = T_{amb}$  and  $RH_A$  measured from ambient air. The wall temperature from (2.11) is used for  $T_C = T_w$  and  $RH_C = 100\%$ .

The difference between  $AH_A$  and  $AH_C$  defines the amount of water condensation. Returning back to the Eqs. (2.14)–(2.18) the following substitution is done for the absolute humidity

$$X_{air\_in} = AH_A / 10^3 \quad \text{and} \quad X_{air\_out} = AH_C / 10^3 \quad (2.24)$$

## 2.5 Model Validation

Experiments are done to collect measurement data for model validation. The experiments fall apart into two parts:

- HIL compressor measurements: A HIL test setup is used to characterize the model parameters of an isolated AC compressor. The preferred items to be measured are the pressure, temperature, and flow of the refrigerant when entering/leaving the compressor. Also the compressor speed and torque is measured to determine its mechanical power.
- Rollerdyne measurements: A climate chamber with heavy duty roller dynamometer is used to estimate the model parameters of the complete AC system. A picture of the climate chamber test setup (with DAF XF EuroVI truck) is shown in Fig. 2.6.

**Fig. 2.6** Validation of AC system with DAF test truck in climate chamber



The pressure and the temperature of the refrigerant are measured at six locations: compressor in/out, condensor in/out, expansion valve in, and evaporator out. The torque and speed of the compressor are measured to determine its mechanical power. The temperature of the airflow is measured before and after the evaporator as well as the condensor. Different experiments are done with ambient conditions:  $10 \leq T_{\text{amb}} \leq 30^\circ\text{C}$ ;  $50 \leq \text{RH} \leq 70\%$ .

### 2.5.1 Validation of Compressor Model

The compressor measurements with the HIL test setup offer insight into the volumetric efficiency  $\eta_{\text{vol}}$  and the compressor efficiency  $\eta_{\text{isen}}$ . Both parameters are measured and stored in a look-up-table as function of compressor speed and charge/discharge ratio. Validation of the compressor torque in (2.9) is done with help of the rollerdyne measurements in the climate chamber. From the measurement data, the following information is used:

- Speed: The speed of the ICE is available and will be used to determine the AC compressor speed (by means of a fixed ratio determined by the pulley).

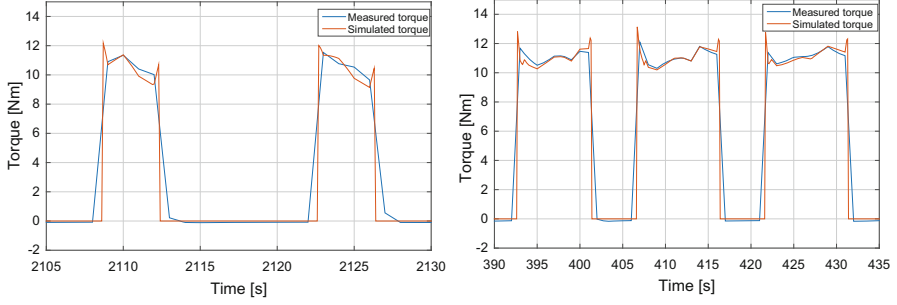


**Fig. 2.7** Validation of compressor torque:  $T_{\text{amb}} = 25^{\circ}\text{C}$  (left) and  $T_{\text{amb}} = 30^{\circ}\text{C}$  (right)

- Torque: A dedicated torque sensor is installed to measure the torque of the AC compressor.
- Pressure: Two pressure sensors are applied to measure the charge and discharge pressure of the compressor.

The compressor torque from (2.9) is plotted against measurement data in Fig. 2.7. Two different use cases are considered for the compressor torque: the left picture shows the situation with ambient temperature  $25^{\circ}\text{C}$ ; the right picture shows the situation with ambient temperature  $30^{\circ}\text{C}$ . The model achieves the best accuracy when the compressor clutch is completely closed (error smaller than 10 %). Less accuracy is achieved during closing and opening of the clutch. This is because the model does not take into account slipping of the clutch.

### 2.5.2 Validation of Thermal AC Model

This section describes the validation of the thermal AC model as derived in Sect. 2.4. A comparison will be made between the air temperature downstream the evaporator and the temperature  $T_w$  estimated by the model (2.11). Before the model validation can start, first an explanation is needed about the measured temperatures in the HVAC.

During the rollerdyne experiments, the temperature downstream the evaporator is measured with nine temperature sensors. These sensors are all mounted on the back-wall of the evaporator, distributed on a  $3 \times 3$  grid. This allows to measure the temperature behind the evaporator at nine different locations in the air channel. For one experiment ( $T_{\text{amb}} = 25^{\circ}\text{C}$ ) these sensor measurements are visualized in Fig. 2.8. It is observed that the air temperature behind the evaporator does not respect a homogenous distribution. For validation of (2.11) only one temperature profile can be used. It is decided to use the temperature sensor with comes closest to the average temperature of all nine sensors.

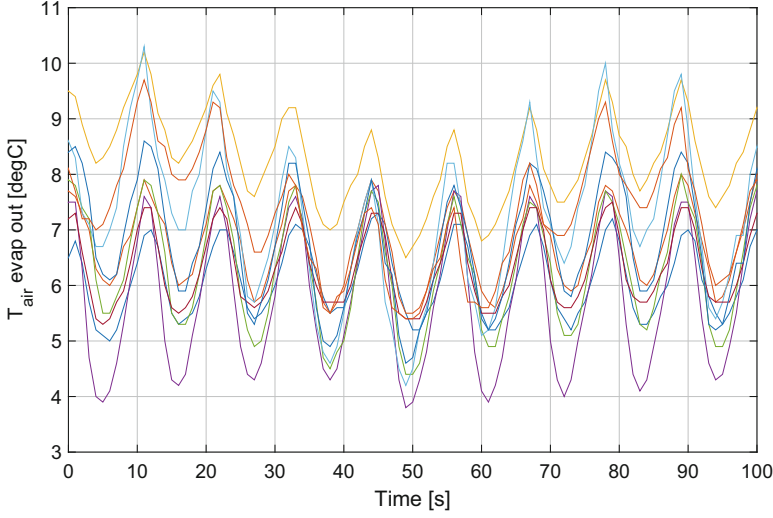


**Fig. 2.8** Measured air temperature downstream evaporator; nine sensors measure temperature distribution over air channel

The next step will be the identification of the model parameters. The rollerdyne experiments are used to identify the model parameters from the thermal equations (2.10)–(2.12). The parameters which will be identified are the heat capacities  $C_w$  and  $C_r$  and the thermal resistance  $R_i$ . The experiment that has been selected to identify these parameters entails a low ambient temperature and low humidity. This ensures that water condensation is avoided in the HVAC and its impact on the heat balance from (2.11) can be neglected (i.e.,  $Q_{\text{water\_liq\_out}} = 0$  and  $Q_{\text{latent}} = 0$ ). The identification toolbox from *Matlab* is used to find the parameters of interest. In particular, a gray-box identification is done by constructing an Output-Error OE model structure. The *Matlab* function *Idgrey* is finally used to calculate  $C_w$ ,  $C_r$ , and  $R_i$ .

Now that the model parameters are identified, the final validation of the thermal model is done. Recall that in this work a pressure model is lacking for the refrigerant R134a. To overcome this problem, the cooling input power  $P_{\text{AC\_cool}}$  in (2.12) is calculated from the enthalpy change in the evaporator, see also [3]. With help of the experimental data, the following approximation has been chosen:

$$P_{\text{AC\_cool}} \approx (h_{\text{evap\_in}} - h_{\text{evap\_out}}) \dot{m}_{\text{R134a}} \quad (2.25)$$

where  $\dot{m}_{\text{R134a}}$  is determined by Eq. (2.3) from the compressor model. The pressure sensors, which are installed before the expansion valve and after the evaporator, are used to estimate the enthalpy  $h_{\text{evap\_in}}$  [J/kg] and  $h_{\text{evap\_out}}$  [J/kg], respectively. Conversion from pressure to enthalpy is done according to the standard pressure-enthalpy diagrams available from literature. In Fig. 2.9 this conversion is visualized

**Fig. 2.9** Static relation between pressure and enthalpy for R134a

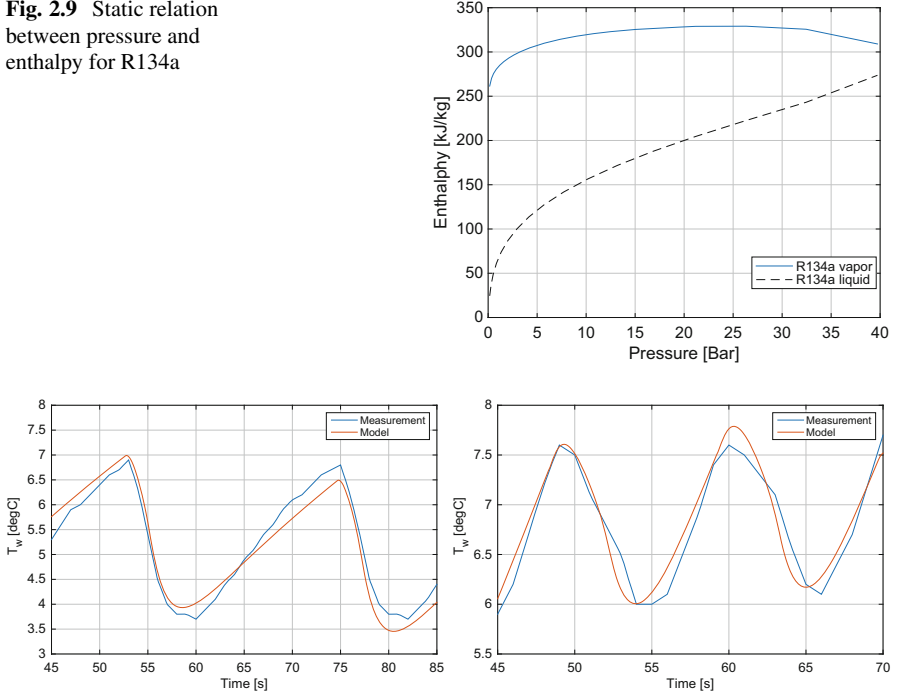


**Fig. 2.10** Validation of evaporator wall temperature:  $T_{amb} = 15^\circ\text{C}$  (left) and  $T_{amb} = 25^\circ\text{C}$  (right)

for refrigerant R134a (data taken from [8]). The refrigerant is assumed to be in liquid phase before the expansion valve, whereas after the evaporator the refrigerant must be in gas form. This way,  $h_{\text{evap\_in}}$  relies on the liquid graph and  $h_{\text{evap\_out}}$  uses the vapor graph.

The final validation of the thermal AC model is done with experiments at a higher temperature to include the verification of the latent heat model. In particular, the experiments with ambient temperature 15 and  $25^\circ\text{C}$  are selected to show the validation results in Fig. 2.10. One can observe that the temperature cycles between fixed boundaries. The exact behavior of these cycles relates to the on/off strategy of the compressor clutch. The compressor clutch strategy, however, is not investigated in this work. Nonetheless, a higher ambient temperature results in a higher load for the AC system and the cycle frequency goes up.

Figure 2.10 also reveals that the AC model, in particular Eq. (2.11), is able to predict the temperature downstream the evaporator. During the on-time of the compressor (where the temperature decreases) as well as during the off-time (where the temperature increases) the model achieves an error smaller than  $0.5^\circ\text{C}$ .

There should be noted that the accuracy of  $T_w$  highly depends on the accuracy of the cooling input  $P_{\text{AC\_cool}}$ . A mismatch in cooling power defined in (2.12) results in drift for the estimated temperature  $T_w$ .

## 2.6 Concluding Remarks

This chapter develops a model for the airco system in heavy duty long haul trucks. Two aspects of the airco model are considered in detail:

- Compressor model: The airco system requests mechanical power, ultimately delivered by the diesel engine of the truck. The compressor model calculates the mechanical power for the situation that the compressor clutch is closed. This model also predicts the massflow of the refrigerant through the compressor, which is used to determine the cooling power in the thermal part of the airco model.
- Thermal AC model: Ambient air cools down when it passes the evaporator. This part of the model estimates the airflow temperature directly behind the evaporator. The model also estimates the humidity of the output air, as well as the amount of water condensation.

Both elements of the model are verified by means of experimental validation. A HIL test-setup is used to collect specific measurement data of the compressor: the volumetric efficiency and the isentropic efficiency. Next, a DAF XF prototype truck is placed in a climate chamber on a roller dynamometer. Experiments at different ambient conditions are done to validate the model. A comparison between the measurement data and the model outputs learns that the following accuracy is established:

- Compressor model: The compressor torque is calculated within 10 % of the measured torque signal. Slipping of the compressor clutch is not considered. During transient situations (i.e., when the clutch closes/opens and the compressor switches on/off) the model loses validity.
- Thermal AC model: The temperature of the airflow leaving the evaporator resembles the measurement data. The temperature of the model deviates less than 0.5 K from the measurement data (considering various ambient conditions).

Future research for this airco model should address the development of a pressure model. Once the model includes a pressure model for the refrigerant, it can be used to develop advanced energy management strategies.

## References

1. C.P. Arora, *Thermodynamics* (McGraw-Hill Education (India) Pvt Limited, Bangalore, 2001)
2. Complete vehicle energy-saving technologies for heavy-trucks (CONVENIENT), (2016), [www.convenient-project.eu](http://www.convenient-project.eu)
3. S.P. Datta, P.K. Das, S. Mukhopadhyay, Effect of refrigerant charge, compressor speed and air flow through the evaporator on the performance of an automotive air conditioning system, in *Proceedings of the 15th International Refrigeration and Air Conditioning Conference*, Purdue, 14–17 July 2014

4. W.O. Forrest, M.S. Bhatti, Energy efficient automotive air conditioning system, in *SAE 2002 World Congress*, Detroit, Michigan, 4–7 March 2002. SAE Technical Paper 2002-01-0229
5. M. Fritz, F. Gauterin, M. Frey, J. Wessling, E. Wohlfarth, R. Oberfell, An approach to develop energy efficient operation strategies and derivation of requirements for vehicle subsystems using the vehicle air conditioning system as an example, in *SAE 2013 World Congress & Exhibition*, Detroit, Michigan, 2013. SAE Technical Paper 2013-01-0568
6. Humidity conversion formulas - calculation formulas for humidity, Technical Report, Vaisala Oyj, Helsinki, Finland, 2013
7. J.T.B.A. Kessels, J.H.M. Martens, P.P.J. van den Bosch, W.H.A. Hendrix, Smart vehicle powernet enabling complete vehicle energy management, in *Proceedings of the IEEE Vehicle Power and Propulsion Conference (VPPC)*, Seoul, Korea, October 2012, pp. 938–943
8. Pressure - enthalpy diagram 134a, Technical Report, INEOS Fluor, Cheshire, 2001
9. S.R. Turns, *Thermodynamics: Concepts and Applications* (Cambridge University Press, Cambridge, 2006)
10. Q. Zhang, M. Canova, Modeling and output feedback control of automotive air conditioning system. *Int. J. Refrig.* **58**, 207–218 (2015)



Automotive Air Conditioning

Optimization, Control and Diagnosis

Zhang, Q.; Li, S.E.; Deng, K.

2016, VIII, 366 p. 162 illus., 139 illus. in color.,

Hardcover

ISBN: 978-3-319-33589-6